Human phonation analysis by 3d aero-acoustic computation

S. Zörner[1,2] M. Kaltenbacher[1] W. Mattheus[3] C. Brücker[3]
[1] *Alps-Adriatic University of Klagenfurt, Chair of Applied Mechatronics*
[2] *Universität Erlangen-Nürnberg, Depart. of Sensor Technology,*
[3] *TU Bergakademie Freiberg, Institut für Mechanik und Fluiddynamik*

Introduction

Phonation is the basis of human voice which needs to be analysed and understood. The airstream through the larynx is throttled by the opening and closing of the vocal folds generating a pulsating flow resulting in a tonal sound. It is the main sound source followed by turbulent flow which generates a random broadband signal. The overall generated sound propagates towards the vocal tract which acts as a sound filter, from which formants are produced.
The fluid simulation is done on a 3d domain with an elliptic formed glottis opening and stiff vocal folds. The fluid data was then exploited to determine the acoustic sources for each time step via Lighthill's analogy. This was then used to simulate the acoustic pressure propagation throughout the domain.

Physical fields

Two different physical fields are dealt with, the fluid mechanics and the acoustics. The fluid flow was simulated in water to make a direct comparison with a developed experimental setup possible [6]. However, the flow data is then transformed to allow for an acoustic computation in air.
For the given flow conditions, the Mach number is below 0.3, so that we can assume an incompressible flow. The governing set of partial differential equations is given by the momentum and mass conservation

$$\rho\frac{\partial\vec{v}}{\partial t}+\rho(\vec{v}\cdot\nabla)\vec{v}+\nabla p-\mu\Delta\vec{v}=0\,, \tag{1}$$

$$\nabla\cdot\vec{v}=0\,, \tag{2}$$

with $\vec{v}$ the flow velocity, p the pressure, ρ the density and μ the dynamic viscosity. The set of equations are solved with the open source solver OpenFOAM [7], which is based on the finite volume-method of second order. The first order time derivative is discretised by the Crank-Nicolson method.

Acoustic field - Aeroacoustics

The acoustic field is calculated in a separate step following the fluid simulation, since we assume that there is no back reaction of the acoustic on the fluid field. With the equation of continuity and momentum Lighthill's equation in pressure form is derived (for details, cf. [4])

$$\frac{1}{c^2}\frac{\partial^2 p'}{\partial t^2}-\Delta p'=\nabla\cdot(\nabla\cdot\mathbf{T}), \tag{3}$$

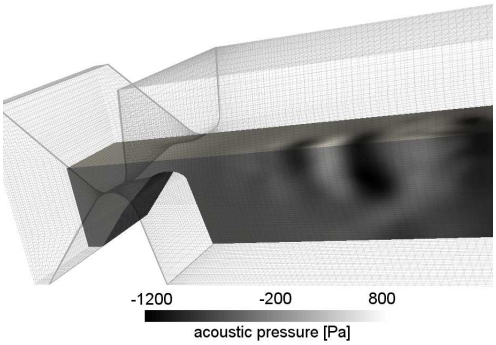

Figure 1: Acoustic pressure distribution along the centre of the computational domain.

with c the speed of sound and $\mathbf{T}$ the Lighthill tensor

$$\begin{aligned} T_{ij} &= \underbrace{\rho_f v_i v_j}_{\text{Reynolds stress}} + \underbrace{\tau_{ij}}_{\text{Viscous stress}} \\ &+ \underbrace{[(p-p_0)-c^2(\rho_f-\rho_0)]\delta_{ij}}_{\text{Heat conduction}}. \end{aligned} \tag{4}$$

Thereby, p' denotes the acoustic pressure, p_0 is the mean pressure, ρ the fluid density and ρ_0 its mean density. It is assumed that no heat conduction takes place and the viscous stress may be neglected [4], therefore an approximation of (4) can be given by

$$T_{ij}\approx\rho v_i v_j. \tag{5}$$

Simulation Setup

As depicted in Figure 1, a 3d domain was chosen with an elliptic formed glottis and an overall size of $20\times20\times60\mathrm{mm}$ [5] which is decomposed into approx. 750 000 elements. In accordance to the experimental setup (see [6]) the physical properties of water are chosen for the flow computation. Furthermore, velocities and frequencies are strongly reduced making experimental measurements easier. Now, to match the results for an air stream through a human sized larynx, we scale the physical quantities by keeping Strouhal number (St), Reynolds number (Re) and Euler number (Eu) constant

$$Re = \frac{v_{mean}^{\text{air}}w^{\text{air}}}{\nu^{\text{air}}}=\frac{v_{\text{mean}}^{\text{water}}w^{\text{water}}}{\nu^{\text{water}}} \tag{6}$$

$$St = \frac{f^{\text{air}}b^{\text{air}}}{v_{\text{mean}}^{\text{air}}}=\frac{f^{\text{water}}b^{\text{water}}}{v_{\text{mean}}^{\text{water}}} \tag{7}$$

$$Eu = \frac{2\Delta p^{\text{air}}}{\rho^{\text{air}}\left(v_{\text{mean}}^{air}\right)^2}=\frac{2\Delta p^{\text{water}}}{\rho^{\text{water}}\left(v_{\text{mean}}^{\text{water}}\right)^2}. \tag{8}$$

dimension	scaling factor (Water→Air)
velocity	45
frequency	135
time	$\frac{1}{135}$
pressure	2
geometric dimension	$\frac{1}{3}$

Table 1: Scaling factors from water to air

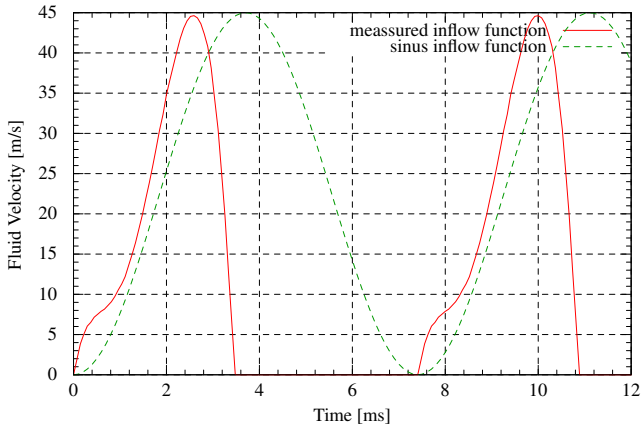

Figure 2: Fluid inflow condition scaled to air.

In (6)-(8) ν^{medium} denotes the kinetic viscosity in the appropriate medium, v_{mean} the mean velocity, $w_{\max}$ the maximal glottis width, f the fundamental frequency of the oscillation, b the thickness of the vocal folds, ρ the density and p the hydrodynamic pressure. The resulting scaling factors for the relevant physical quantities are listed in Tab.1 (for details see [6]). In this paper referred physical quantities are regarded to be in air.

Boundary conditions

In the fluid simulation we apply no-slip boundary conditions on all sides of the domain, except the inflow and outflow. At the inflow Dirichlet condition for the fluid velocity were set. Thereby, two different inflow conditions were analysed, a sinusoidal and an inflow condition as depicted in Figure 2 with a period of $1/135$ s , which has been measured in the experimental setup with moving vocal folds and a fixed pressure gradient. At the outflow a homogeneous Dirichlet conditions for the hydrodynamic pressure is set.
For the acoustic computation we apply absorbing boundary conditions of first order at the surfaces of inflow and outflow [1, 2]. This will make sure, that no acoustic wave impinging these boundaries will be reflected back to the computational domain. All other surfaces were set to hard, acoustic reflecting walls.

Numerical Method

The wave equation (3) is discretised using the Finite-Element method (FEM). As a rule of thumb 20 linear finite elements should be used per wave length [3]. Since the maximum frequency encountered in this application is about 8kHz the fine grid of the CFD computation is more than sufficient for acoustics.

Computational acoustics

The FEM requires the governing equations (3) in a weak formulation. Thereby, (3) needs to be multiplied by an appropriate test function $\phi \in H_0^1(\Omega)$ and be integrated over the computational domain Ω, giving

$$\int_\Omega \frac{1}{c^2}\frac{\partial^2}{t^2}p'\phi \,\mathrm{d}x + \int_\Omega \nabla p' \cdot \nabla\phi \,\mathrm{d}x + \int_{\Gamma_{\text{io}}} \frac{1}{c}\frac{\partial}{\partial t}p'\phi \,\mathrm{d}x = -\int_\Omega \nabla \cdot T \cdot \nabla\phi \,\mathrm{d}x. \quad (9)$$

An advantage of the FEM regarding Lighthill's analogy is the order reduction of the spatial derivative of the Lighthill tensor due to the integration by parts. The boundary integral in (9) arises from partial integration together with the absorbing boundary condition [3] given by

$$\nabla p' \cdot \vec{n} = -\frac{1}{c}\frac{\partial}{\partial t}p'.$$

The infinite-dimensional space is replaced by finite-dimensional subspace $V_h \subset H_0^1$ and the pressure is approximated by

$$p'(t,x) \approx p'_h(t,x) = \sum_{i=1}^{N} p'_i(t)\psi_i(x)$$

with $\{\psi_1, \ldots, \psi_N\}$ a basis of V_h and N the number of FE nodes in the computational domain. With an appropriate set of basis function the test functions are chosen from this set, resulting in a matrix vector notation of (9)

$$\boldsymbol{M}\ddot{\boldsymbol{p}} + \boldsymbol{K}\boldsymbol{p} = \boldsymbol{F}. \quad (10)$$

In (10) $\boldsymbol{M}$ denotes the mass matrix and $\boldsymbol{K}$ the stiffness matrix, The discrete acoustic pressure is denoted as $\boldsymbol{p}$ and its second derivative as $\ddot{\boldsymbol{p}}$ which is discretised in time by the Newmark scheme. The inhomogeneous part $\boldsymbol{F}$ is the finite element form of the approximated Lighthill tensor (5).

Acoustic Results

The acoustic signal obtained from the numerical simulation with different inflow conditions are provided in Figure 3. For all different setups, the main frequency of the inflow velocity (135 Hz) is also found in the acoustic sound. Furthermore, harmonics are dominant with a lower amplitude as the main frequency. This acoustic spectrum is superimposed by a broadband sound. The stochastically generated sound varies in space, which has the highest amplitude a diameter downstream the glottis. At this point the flow is quite turbulent compared to the point at outflow or at the glottis.
A further simulation has been done with a fluid flow, which was phase averaged over 30 cycles. Therewith, all cycle-to-cycle fluctuations in the fluid field is removed. The impact on the acoustic sound was that only the main frequency and harmonics remain, as depicted in Figure 3b. Stochastic parts are not present any more.
The higher slope of the measured inflow function results in higher acoustic pressure compared to the sinusoidal inflow function as can be seen in Figure 3c.

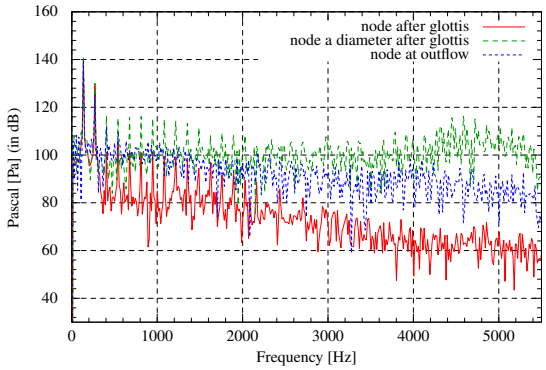

(a) Acoustic frequency spectrum of a sinusoidal inflow condition

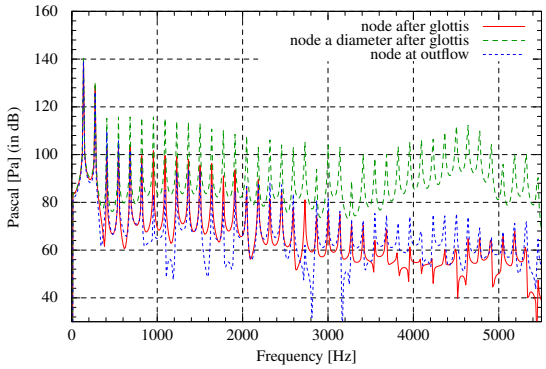

(b) Acoustic frequency spectrum of a sinusoidal inflow condition. The fluid field is phased averaged over 30 periods.

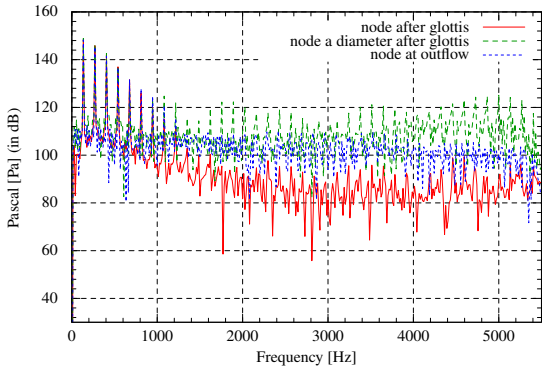

(c) Acoustic frequency spectrum of a sawtooth inflow condition.

Figure 3: acoustic frequency of different fluid inflow conditions.

Conclusion

A computational method has been introduced describing the aerodynamics in a stiff larynx model. Different inflow conditions have been applied to give an insight in the resulting acoustic sound. By phase averaging of the fluid flow the turbulent component could be associated to the broadband sound, while the pulsating flow is responsible for the main frequencies. In a last computation, we have calculated the acoustic sound based on the measured inflow conditions (see Figure 2. A next step is to apply moving vocal folds, which thereby influence the fluid rate and turbulent flow.

Acknowledgements

Funding by the German Research Foundation (Deutsche Forschungsgemeinschaft, DFG) is gratefully acknowledged.

References

[1] Robert Clayton and Björn Engquist. Absorbing boundary conditions for acoustic and elastic wave equations. *Bulletin of the Seismological Society of America*, 67(6):1529–1540, 1977.

[2] Björn Engquist and Andrew Majda. Absorbing boundary conditions for the numerical simulation of waves. *Mathematics of Computation*, 31(139):629–651, 1977.

[3] M. Kaltenbacher. *Numerical Simulation of Mechatronic Sensors and Actuators*. Springer, Berlin, 2. edition, 2007.

[4] M. J. Lighthill. On sound generated aerodynamically I. General theory. *Proceedings of the Royal Society of London*, 1951.

[5] X. Pelorsonf, A. Hirschberg, R. R. vanHassel, and A. P. J. Wijnands abd Y. Auregan. Theoretical and experimental study of quasisteady-flow separation within the glottis during phonation. application to a modified two-mass model. *Journal of the Acoustical Society of America (JASA)*, 1994.

[6] M. Triep, Ch. Brücker, and W. Schröder. High-speed piv measurements of the flow downstream of a dynamic mechanical model of the human vocal folds. *Experiments in Fluids*, 2005.

[7] H. G. Weller, G. Tabor, H. Jasak, and C. Fureby. A tensorial approach to computational continuum mechanics using object-oriented techniques. *Computers in Physics*, 12, 1998.